

## Original Paper

# Potassium status and availability in three Indian soils as determined by 60 extractions with 1 M CaCl<sub>2</sub>

Debarup Das  and Mandira Barman 

Division of Soil Science and Agricultural Chemistry, ICAR-Indian Agricultural Research Institute, New Delhi-110012, India

### Abstract

Long-term field experiments have shown that continuous potassium (K) removal depletes soil K levels and alters clay minerals, leading to significant fertility decline. This study aimed to replicate similar findings through a laboratory investigation. The objectives included examining K-release behavior in three soils under continuous K depletion, and analyzing changes in available and non-exchangeable K, K-fixation capacity, and clay minerals. Additionally, the study sought to identify the clay minerals involved in K release and assess the feasibility of simulating long-term cultivation effects through laboratory leaching. A red soil (Alfisol), a black soil (Vertisol), and an alluvial soil (Entisol) from three states of India were each leached 60 times with 1 M CaCl<sub>2</sub>. The K released after each step was measured. The NH<sub>4</sub>OAc-K, non-exchangeable K by nitric acid (NEK-HNO<sub>3</sub>), and sodium tetraphenyl borate (NEK-NaTPB) methods (5 min), clay mineralogy, and K-fixation capacity before and after the 60× leaching were assessed. Total K released over 60× leaching followed the order black > alluvial > red soil. The constant rate of K release was the same for all three soils. The NH<sub>4</sub>OAc-K showed a significant decrease in all soils, while NEK-HNO<sub>3</sub> did not change significantly. The NEK-NaTPB decreased significantly, while the K-fixation capacity increased significantly in the red and the alluvial soils. The K depletion caused a noticeable decline in the relative abundance of 2:1 mixed-layer minerals in the red and the black soils and of illite in the alluvial soil. The trioctahedral illite became depleted in all three soils. The center of gravity of the X-ray diffraction peaks of the 2:1 clay minerals was reduced slightly due to K depletion, which contradicts current beliefs. Sixty leachings of soils with 1 M CaCl<sub>2</sub> could only partially simulate the long-term, cultivation (without K fertilization)-induced changes in soil K fertility and clay minerals.

**Keywords:** clay mineralogy; non-exchangeable potassium; potassium depletion; potassium fixation; sequential leaching; X-ray diffraction

(Received: 11 April 2024; revised: 21 October 2024; accepted: 17 February 2025)

### Introduction

Plants need potassium (K) in large quantities for growth and development. It is crucial for biomolecule synthesis, enzyme activation, osmotic regulation, ionic balance, stress resistance, nutrient-use efficiency, and in improving the overall quality of plants (Weil and Brady, 2017). Besides its essential role in plants, the stability of mica, illite, and some mixed-layer minerals (MLMs) in soil relies on the K input–output balance, underscoring its importance for soil health (Das et al., 2019a; Das et al., 2021). Hence, proper K management for agricultural purposes is essential in countries such as India, where all K for fertilization purposes is imported. A recent review by Das et al. (2022) revealed that India's fertilization has focused on nitrogen (N) and phosphorus (P), largely ignoring K. This oversight has led to net K removal in intensively cultivated soils, depleting exchangeable and non-exchangeable K pools and affecting clay minerals and K-fixation capacity over time (Das et al., 2018; Das et al., 2019a;

Das et al., 2021). Continuous K removal has negatively affected various soil properties, as reported in greenhouse and field studies from other countries (e.g. Biliás and Barbayiannis, 2017; Moterle et al., 2016; Li et al., 2017a; Li et al., 2017b; Liu et al., 2020; Han et al., 2021; Chen et al., 2023). Understanding soil K dynamics, clay mineral changes, and K-fixation potential is essential for developing soil-specific K-management strategies. However, conducting long-term field or greenhouse studies to understand soil K dynamics is not always feasible, as they require significant time and effort. Quick and simple methods for generating data on soil K dynamics are required.

Repeated leaching of soils with a suitable solution may provide valuable data on K dynamics, similar to long-term field or greenhouse studies. Unlike traditional methods that may cause K release through shaking or boiling, leaching allows for the observation of changes in K fractions, fixation capacity, and clay minerals without particle aberration. Sufficient leaching may induce changes akin to those seen in field experiments, making the resulting data significant. Achieving substantial K depletion will require multiple leaching cycles; the more cycles conducted, the greater the K depletion. However, excessive leaching can become cumbersome and time-consuming. Therefore, the number of leaching cycles should be optimized to ensure adequate K

**Corresponding authors:** Debarup Das and Mandira Barman; Emails: [debarup.das@icar.gov.in](mailto:debarup.das@icar.gov.in); [mandira.barman@icar.gov.in](mailto:mandira.barman@icar.gov.in)

**Cite this article:** Das D., & Barman M. (2025). Potassium status and availability in three Indian soils as determined by 60 extractions with 1 M CaCl<sub>2</sub>. *Clays and Clay Minerals* 73, e14, 1–13. <https://doi.org/10.1017/cmn.2025.6>

depletion without becoming unmanageable, ideally exceeding the point where K release reaches a constant rate.

The next challenge is selecting an appropriate extraction solution. Ammonium acetate ( $\text{NH}_4\text{OAc}$ ) or any ammonium salt is unsuitable for repeated extractions, as  $\text{NH}_4^+$  can block the entry points of K-bearing 2:1 minerals, limiting K release severely after removing soil solution and surface-adsorbed K (Paul et al., 2024). Conversely, using acids such as  $\text{HNO}_3$  or  $\text{HCl}$  for repeated extractions leads to unavoidable mineral dissolution (Li et al., 2015; Najafi-Ghiri et al., 2019; Najafi-Ghiri et al., 2023). Low-molecular-weight organic acids may also release some K through mineral dissolution, aside from cation exchange, if added repeatedly in high concentrations (Hashemi and Najafi-Ghiri, 2024). A concentrated solution of a neutral salt, such as  $\text{CaCl}_2$ , is a better option as it does not reduce soil pH. As the most abundant ion in slightly acidic to alkaline and calcareous soils,  $\text{Ca}^{2+}$  influences K release from soil solids significantly (Barman and Das, 2024). Furthermore, soil K extracted with 0.01 M or stronger  $\text{CaCl}_2$  correlates well with plant K uptake (Bell et al., 2021a; Cheng et al., 2023; Paul et al., 2024), although concentrations must exceed 0.01 M for significant K depletion.

The neutral normal  $\text{NH}_4\text{OAc}$ -extractable K (soil solution K + exchangeable K) is the most frequently measured variable to assess the K status of a soil (Das et al., 2022). Declines of ~49, ~46, and ~29% were observed by Das et al. (2019a, 2021) in  $\text{NH}_4\text{OAc}$ -K under fertilization with N and P but not K (relative to adjacent uncultivated land) in a red soil (Jharkhand, India), a black soil (Madhya Pradesh, India), and an alluvial soil (New Delhi, India), respectively, after 41–42 years of cultivation. Due to the dynamic equilibrium of soil K forms, non-exchangeable K (NEK) can counteract decreases in exchangeable and solution K, leading researchers to include it in K-dynamics studies (Srinivasarao et al., 2014; Das et al., 2019a; Das et al., 2021; Das et al., 2022). Traditionally assessed using the boiling  $\text{HNO}_3$  method (Page et al., 1982), recent studies suggest that sodium tetrathanylborate ( $\text{NaTPB}$ ) provides a more accurate estimate of NEK.  $\text{NaTPB}$  extraction relies mainly on cation exchange without dissolving minerals, better simulating plant-root action (Li et al., 2015; Wang et al., 2016). The extraction time with  $\text{NaTPB}$  can vary, based on requirement, e.g. 1 or 5 or 15 min for routine analysis of plant-available NEK (Cox et al., 1999); 1 h for NEK occupying interlayer frayed-edge sites of 2:1 minerals and was considered plant-available NEK by Carey and Metherell (2003); 16 h for plant-available reserve K (Jackson, 1985a); 24 h or 1 day for NEK held in high-energy interlayer sites apart from that extracted in 1 h, a large part being not available to plants in short- to medium-term (Carey and Metherell, 2003; Das et al., 2019a); 7 days for potentially available illite K (Cox et al., 1999; Biliias and Barbayiannis, 2019); and 10–20 days for complete extraction of entire NEK reserve, which may account for 21–56% of total K of soils (Wang et al., 2016). Cox et al. (1999) recommended 5 min for routine NEK assessment by  $\text{NaTPB}$ , finding that ~80% of K extracted in that time is plant-available. Later, Biliias and Barbayiannis (2019) observed a better correlation of critical available K in soil with  $\text{NaTPB}$ -K (5 min) than with  $\text{NaTPB}$ -K (1 min) or  $\text{NH}_4\text{OAc}$ -K. Changes of +3.7, –18.9, and –14.6% were recorded (Das et al., 2019a; Das et al., 2021) in  $\text{HNO}_3$ -extracted NEK under NP fertilization without K (at 0–15 cm depth, compared with adjacent uncultivated land) in a red soil (Ranchi, India), black soil (Jabalpur, India), and an alluvial soil (New Delhi, India), respectively, after 41–42 years of cultivation. The corresponding changes in  $\text{NaTPB}$  (5 min)-extracted NEK were –8.8, –19.3, and –24.5% (Das, 2018).

In a 45-year field experiment on an illite-dominated alluvial soil in eastern India, Das et al. (2018) identified K-fixation capacity as a sensitive soil property affected by long-term cultivation and K fertilization under a rice-rice cropping system (rice crop was grown twice a year, once in the wet season from July to November, and once in the dry season from January to May). The K-fixation capacity can vary significantly with clay mineralogy and K input–output budgets (Das et al., 2018; Portela et al., 2019; Shakeri and Abtahi, 2020). Changes in K-fixation capacity relative to K removal may indicate the reversibility of K depletion. In Sweden, Simonsson et al. (2009) found that changes in K-fixation capacity accounted for 0–70% of the K added to or removed from the soil in five long-term experiments. As several clay minerals are involved in K release and fixation, they are crucial in soil K dynamics and show changes under severe K depletion (Li et al., 2017b; Das et al., 2019a; Das et al., 2022). X-ray diffraction (XRD) is the most widely used technique for studying clay minerals. Whilst clay-mineral alterations due to K depletion could be elusive, variables such as the relative peak area, the center of gravity of the XRD peaks of 2:1 clay minerals ( $cg$ ), and the ratio of first-order and second-order diffraction of mica or illite (001/002) obtained from XRD patterns might be able to highlight subtle changes effectively (Pal et al., 2001; Barré et al., 2007; Li et al., 2017b; Yanai et al., 2023).

Considering these facts, a laboratory study was conducted in which a red soil (acidic), a black soil (slightly alkaline), and an alluvial soil (calcareous) from three Indian states were leached 60 times (60 $\times$ ) each with 1 M  $\text{CaCl}_2$  and changes in various soil properties were observed. These three soils belong to the dominant soil types of India. The objectives were: (1) to study the K-release behavior of the three soils under continuous K depletion caused by successive leaching in the laboratory; (2) to assess the effect of K depletion on available and non-exchangeable K, K-fixation capacity, and clay minerals; (3) to identify the clay minerals involved in K release under continuous K depletion; and (4) to evaluate the feasibility of a laboratory leaching study to simulate long-term, cultivation-induced changes in K fractions, fixation capacity, and clay minerals of the three soils.

## Materials and methods

### Collection and characterization of soils

Surface soil (0–15 cm) was collected from uncultivated, unfertilized lands at the three sites (Table 1). Soils from 12 spots at each site were grouped into three composite samples. The samples were air-dried, ground with a wooden pestle and mortar, and passed through a 2-mm sieve. Soil was treated with 1 M sodium acetate ( $\text{NaOAc}$ ) at pH 5 to remove free carbonates, 30% hydrogen peroxide ( $\text{H}_2\text{O}_2$ ) to oxidize organic matter, sodium citrate-bicarbonate-dithionite to remove iron oxides, and finally with 10% sodium hexametaphosphate [ $(\text{NaPO}_3)_6$ ] followed by stirring using a laboratory stirrer to yield a dispersed suspension (Lab Stirrer RQ-5 Plus, Remi Elektrotechnik Ltd, India) (Jackson, 1985b; Prasad et al., 2019). Sand, silt, and clay proportions were determined in the dispersed suspension by the hydrometer method (Bouyoucos, 1962), and soil textural class by the USDA Soil Texture Calculator (<https://www.nrcs.usda.gov/resources/education-and-teaching-materials/soil-texture-calculator>). The pH and electrical conductivity (EC) were determined in separate 1:2.5 soil:water suspensions using a digital pH/conductivity/TDS/ $^{\circ}\text{C}/^{\circ}\text{F}$ -meter (PC 510, Eutech Instruments Pte Ltd, UK) (Jackson, 1973). The cation exchange capacity (CEC) was

**Table 1.** Details of soil collection site and some physicochemical properties of the experimental soils

Soil characteristics	Red soil	Black soil	Alluvial soil
Location	Jharkhand (23°26'49"N 85°18'45"E, 641 m above mean sea level)	Madhya Pradesh (23°12'38"N 79°55'36"E, 404 m above mean sea level)	Bihar (25°58'N, 85°40'E, 53 m above mean sea level)
Taxonomy	Typic Haplustalf	Typic Haplustert	Calciorthent
Texture	Sandy clay loam (60.1% sand, 15.3% silt, 24.6% clay)	Clay (25.1% sand, 17.6% silt, 57.3% clay)	Loam (41.1% sand, 35.8% silt, 23.1% clay)
pH (soil:water, 1:2.5)	4.83	7.60	8.37
Electrical conductivity (EC, soil:water, 1:2.5, dS m <sup>-1</sup> )	0.07	0.19	0.57
Cation exchange capacity (CEC, cmol [p+] kg <sup>-1</sup> )	8.20	42.1	12.1
Organic carbon (%)	0.37	0.52	0.45
Free CaCO <sub>3</sub> (%)	n/d	2.42	33.8

n/d = not detected.

determined by the sodium acetate method at pH 7.0 (Sumner and Miller, 1996; Das et al., 2019b), organic carbon (OC) by wet oxidation (Walkley and Black, 1934), and free calcium carbonate (CaCO<sub>3</sub>) by acid titration (Page et al., 1982).

### Successive leaching of soils

A laboratory experiment was conducted with the three soils (Table 1). Three replications of each soil were taken for the leaching study. For each replication, a 100 g soil sample was placed on a Whatman No. 1 filter paper fitted over a plastic funnel placed on top of a 250 mL volumetric flask and leached 60 times with 250 mL portions of 1 M CaCl<sub>2</sub>. In each case the funnel was covered with parafilm to prevent drying, and was removed only when adding more CaCl<sub>2</sub>. The leachate collected in a volumetric flask after each leaching step was made up to 250 mL with 1 M CaCl<sub>2</sub> solution, and the K concentration was determined with a flame photometer ( $\mu$ Controller based Flame Photometer Type-128, Systronics India Ltd, India). As the volume of leachate collected after each step was not constant and also unmeasurable, the volume after leachate collection at every step was made to a fixed value of 250 mL so that the amount of K in terms of milligrams of K per kilogram of soil could be directly computed from the K concentration in the final 250 mL solution and the volume (i.e. 250 mL). After the 60th leaching step, soils were air-dried in shade and ground to pass through a 2-mm sieve for further analysis.

### Soil analysis

Before and after the leaching experiment, all three replications of the processed soils were analysed for available K with 1 M NH<sub>4</sub>OAc, pH 7 (Hanway and Heidel, 1952). Non-exchangeable K was

determined by two methods: (1) NEK-HNO<sub>3</sub>: K extracted by boiling for 10 min with 1 M HNO<sub>3</sub> minus the NH<sub>4</sub>OAc-K (Page et al., 1982); and (2) NEK-NaTPB: NH<sub>4</sub>OAc-K subtracted from the K extracted for 5 min by NaTPB following the method of Cox et al. (1999) with some modifications in the quenching solution and heating process suggested by Wang et al. (2016). The K-fixation capacity was determined in the soils before and after the leaching experiment. This was achieved by adding 1000 mg of K kg<sup>-1</sup> soil (10 mL of 500 mg K L<sup>-1</sup> solution made of KCl was added to 5 g of soil) and extraction of K with neutral 1 M NH<sub>4</sub>OAc (maintaining soil:solution ratios of 1:10) just after adding the K and after 10 wetting–drying cycles (a single addition of KCl and nine additions of 10 mL of distilled water, and drying at 70±2°C each time) (Jackson, 1973). The K in different extracted solutions was determined by a flame photometer and the K-fixation capacity was calculated using the following equation:

$$K_{\text{fix}} = K_{\text{aa}} - K_{\text{aa,wd}} \quad (1)$$

where  $K_{\text{fix}}$  denotes K-fixation capacity (mg K per kg of soil),  $K_{\text{aa}}$  indicates the NH<sub>4</sub>OAc-extractable K just after adding the KCl solution, and  $K_{\text{aa,wd}}$  represents the NH<sub>4</sub>OAc-extractable K after 10 wetting–drying cycles. The addition of such significant amounts of K (1000 mg K kg<sup>-1</sup> soil) during determination of K-fixation capacity was necessary to ensure that the soils reached their maximum capacity to fix K. Another aim was to establish the increase in a soil's K-fixation capacity after significant depletion of its reserve K.

The three replicate soil samples for each site were pooled together in equal proportions and mixed thoroughly to get a homogeneous composite sample, and used for separation of clay particles (<2  $\mu$ m) following standard procedure (Jackson, 1985b; Das and Datta, 2019). Briefly, soil was treated with 1 M NaOAc at pH 5 for the removal of free carbonates and to make the soils acidic, which were then treated with 30% H<sub>2</sub>O<sub>2</sub> to oxidize organic matter, followed by washing three times with 1 M NaOAc (pH 5), twice with 95% methanol, and twice with 1 M NaOAc (pH 7) to raise the pH to near 7.0. Iron oxides were removed from the soils with sodium citrate-bicarbonate-dithionite treatment described by Mehra and Jackson (1960). The soil was then dispersed by adding a pinch of Na<sub>2</sub>CO<sub>3</sub> and a large amount of water to make the suspension volume ~2.5 L in a tall-form Pyrex glass bottle (see Fig. S1 in the Supplementary material). The suspension was agitated for ~30 s and kept still for 16 h, after which the upper 20 cm suspension containing only clay particles was separated by siphoning. This process of adding distilled water, agitation of the bottle containing the suspension, and siphoning of the upper 20 cm suspension after 16 h of standing was repeated until all the clay particles were separated. The clay separation was done separately for unleached and leached (60 $\times$ ) soils. The clays were made homo-ionic separately with Mg and K. The XRD analysis was done using a Philips X-ray diffractometer (X-ray generator: PW 1729, and diffractometer control: PW 1710; Philips, The Netherlands) on oriented, Mg-saturated glycerol-solvated clays (Mg<sub>gly</sub>), and K-saturated clays after air-drying ( $K_{\text{air}}$ ) and heating at 550°C for 2 h ( $K_{550}$ ). Ni-filtered CuK $\alpha$  radiation ( $\lambda$ , 0.1542 nm) was used at a scanning speed of 1.5°2 $\theta$  min<sup>-1</sup>, with a scanning step size of 0.1°2 $\theta$  over the range 4–15°2 $\theta$  (for  $K_{\text{air}}$  and  $K_{550}$ ) or 4–30°2 $\theta$  (for Mg<sub>gly</sub>). Clay minerals were identified based on peak positions (Jackson, 1985b; Das and Datta, 2019). The 4–15°2 $\theta$  part (this range was chosen to avoid any second-order peak) of the Mg<sub>gly</sub> XRD patterns was deconvoluted into component peaks with the

'fit profile' function of automated powder diffractometer software (APD software, Philips, The Netherlands) following Datta (1996). For deconvolution, a number of profiles (each corresponding to a particular mineral group), approximate peak positions, intensity, full width at half-maximum, and the background were chosen to fit the observed patterns. The parabolic background was chosen from three options: constant, linear, and parabolic, as it overlapped best with the observed background in the XRD patterns. The number of initial profiles varied from 5 to 8 based on the number, position, and shape of the peaks in the observed patterns, and the different minerals identified earlier for similar soils (Das et al., 2019a; Das et al., 2021; Datta et al., 2020; Paul et al., 2024). The program fits Pseudo-Voight functions to the observed patterns based on the selections made. Repeated iterations were performed to ensure the fitted profile matched the observed patterns as closely as possible, yielding a  $\chi^2 < 0.5$ . The deconvolution process enabled estimating areas under the component peaks. Relative peak area (in %) was calculated as 100 times the ratio of a specific peak area ( $a_i$ ) to the total area ( $\sum a_i$ ). The peak heights of the 001 and 002 reflections of illite ( $\sim 10.1$  and  $\sim 4.99$  Å, respectively) were obtained from  $Mg_{gly}$  XRD patterns with the 'peak search' function of the APD software. The 001/002 ratio indicated the trioctahedral component's relative abundance (Pal et al., 2001). The center of gravity of the XRD peaks of the 2:1 clay minerals was determined as per Barré et al. (2007):

$$cg = \frac{\sum_1^n (a_i \times p_i)}{\sum_1^n a_i} \quad (2)$$

where  $a_i$  is the area under the peak,  $p_i$  (in nm) is the peak position, and  $n$  is the number of peaks with  $p_i \geq 1$  nm.

### Statistical analysis

The values of total K released by the soils after 60× leaching were subjected to a one-way analysis of variance for comparison of the three soil types using the 'agricolae' package of R (Mendiburu, 2023). Paired *t*-tests (two-tailed at 5% significance level) were conducted to compare initial soils and soils after 60× leaching for  $NH_4OAc$ -K,  $NEK-HNO_3$ ,  $NEK-NaTPB$ , and K-fixation capacity for each soil type. The *t*-tests were performed using the 'rstatix' package of R (Kassambara, 2023).

## Results

### Physicochemical properties of the soils

The experimental soils varied widely regarding physicochemical properties (Table 1). The red soil was acidic, the black soil was slightly alkaline, and the alluvial soil was highly calcareous (free  $CaCO_3$  33.8%). All three soils were non-saline. The red soil had a sandy clay loam texture; the black soil was clay textured; and the alluvial soil had a loam texture. Due to very large clay contents and similar organic contents, the black soil showed the greatest CEC ( $42.1 \text{ cmol}_c \text{ kg}^{-1}$ ), followed by the alluvial soil ( $12.1 \text{ cmol}_c \text{ kg}^{-1}$ ) and the red soil ( $8.20 \text{ cmol}_c \text{ kg}^{-1}$ ). The black soil showed the greatest OC values (0.52%) followed by the alluvial soil (0.45%) and the red soil (0.37%).

### Potassium released from the soils

The K released per extraction generally decreased with more extractions for black soil (Fig. 1a). For red and calcareous alluvial soils, K release decreased up to the third extraction, increased further slightly until the seventh extraction, then decreased again. The K release from black soil was greater than the other two up to 16 extractions. From the 17th to the 25th extractions, K release was similar across all three soils. Afterward, calcareous alluvial soil released more K until the 34th extraction, beyond which differences among soils were negligible. Overall, all three soils released decreasing amounts of K with extractions, except for occasional inconsistent increases. Cumulative K-release curves were initially steep, then flattened with increasing extractions (Fig. 1b). Total K released after 60 extractions was greatest in black soil ( $235 \text{ mg kg}^{-1}$ ), which was significantly greater than that in alluvial soil ( $198 \text{ mg kg}^{-1}$ ), which in turn was significantly greater than that in the red soil ( $185 \text{ mg kg}^{-1}$ ).

### Changes in $NH_4OAc$ -K, $NEK-HNO_3$ , and $NEK-NaTPB$ due to K depletion

The initial  $NH_4OAc$ -K was the greatest in the black soil ( $107 \text{ mg kg}^{-1}$ ), followed by the red ( $53 \text{ mg kg}^{-1}$ ) and the alluvial ( $32 \text{ mg kg}^{-1}$ ) soils (Fig. 2a). In all soils,  $NH_4OAc$ -K was significantly reduced due to K depletion by 60× leaching. The largest percentage decline from the initial value was in alluvial soil (37.5%), followed closely by black soil

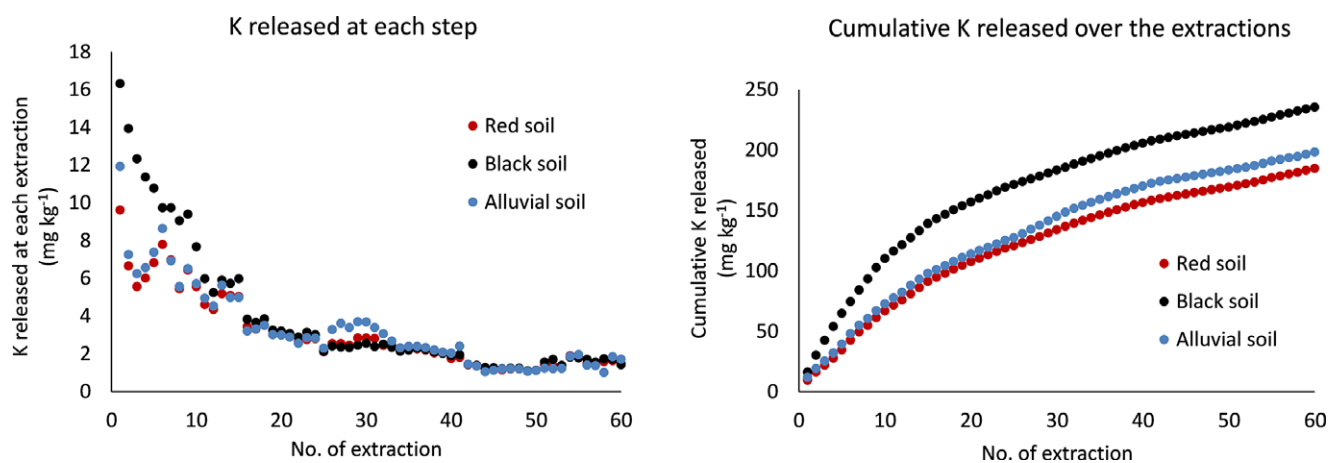


**Figure 1.** (a) K release at each of the 60× leaching steps; and (b) cumulative amount of K released after 60× leaching steps from red, black, and alluvial soils.

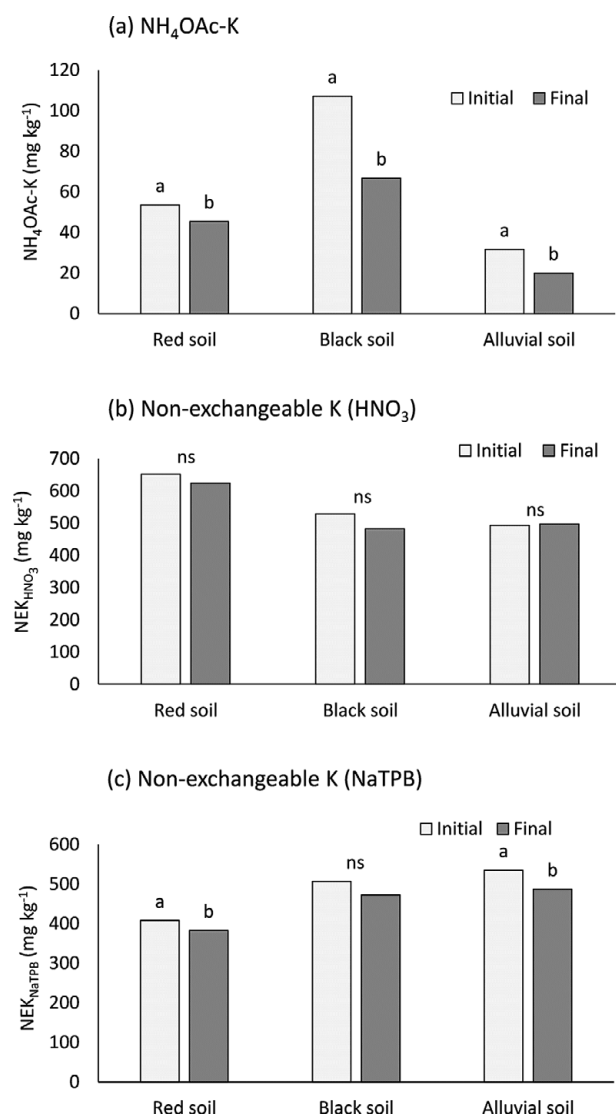


**Figure 2.** (a)  $\text{NH}_4\text{OAc-K}$ , (b)  $\text{NEK-HNO}_3$ , and (c)  $\text{NEK-NaTPB}$ , in 'initial' (before 60 $\times$  leaching) and 'final' (after 60 $\times$  leaching) soils; for a given soil in each figure, 'initial' and 'final' columns with different lower case letters indicate significant ( $p < 0.05$ ) difference between 'initial' and 'final' soils based on paired  $t$ -test (two-tailed); ns = non-significant ( $p > 0.05$ ). Comparison was not made among the three soils.

**Table 2.** Relative change in soil K pools and K-fixation capacity due to K-depletion induced by 60 $\times$  leaching with 1 M  $\text{CaCl}_2$

Soil	Percentage change over initial*			
	$\text{NH}_4\text{OAc-K}^\ddagger$	$\text{NEK-HNO}_3$	$\text{NEK-NaTPB}$	K-fixation capacity
Red soil	-15.1	-4.1	-6.1	36.3
Black soil	-37.4	-8.7	-6.7	-2.9
Alluvial soil	-37.5	0.8	-9.0	20.6

\*Percentage change over initial = [(value after 60 $\times$  leaching - value for initial soil)  $\div$  value for initial soil]  $\times 100$ ;

$^\ddagger\text{NH}_4\text{OAc-K}$ :  $\text{NH}_4\text{OAc}$  extractable K in soil;  $\text{NEK-HNO}_3$ : Non-exchangeable K of soil extracted by boiling nitric acid;  $\text{NEK-NaTPB}$ : Non-exchangeable K of soil extracted by sodium tetraphenyl borate in 5 min.

(37.4%), and least in red soil (15.1%) (Table 2). However, the absolute decline was greatest in black soil (40 mg kg<sup>-1</sup>), followed by alluvial soil (12 mg kg<sup>-1</sup>), and lowest in red soil (8 mg kg<sup>-1</sup>).

The initial amounts of  $\text{NEK-HNO}_3$  in the red, black, and alluvial soils were 651, 528, and 493 mg kg<sup>-1</sup>, respectively (Fig. 2b). The  $\text{NEK-HNO}_3$  showed no significant change due to K depletion in any soil: -4.1, -8.7, and only 0.8% in red, black, and alluvial soils, respectively, after 60 $\times$  leaching (Table 2). Unlike  $\text{NEK-HNO}_3$ , initial  $\text{NEK-NaTPB}$  was greatest in alluvial soil (535 mg kg<sup>-1</sup>), followed by black soil (507 mg kg<sup>-1</sup>), and least in red soil (408 mg kg<sup>-1</sup>) (Fig. 2c). Potassium depletion by 60 $\times$  leaching reduced  $\text{NEK-NaTPB}$  significantly in red and alluvial soils, but not in black soil. Relative to initial content, the  $\text{NEK-NaTPB}$  was decreased by 6.1, 6.7, and 9% in the red, black, and alluvial soil, respectively (Table 2).

### Clay mineralogy of the soils before leaching

The clay minerals were identified from XRD patterns of oriented  $\text{Mg}_{\text{gly}}$ ,  $\text{K}_{\text{air}}$ , and  $\text{K}_{550}$  clay specimens. The pattern for  $\text{Mg}_{\text{gly}}$  of the red soil showed a peak at 14.6 Å, which was absent from  $\text{K}_{\text{air}}$  or  $\text{K}_{550}$  (Fig. 3), indicating expandable 2:1 minerals capable of collapsing after K-saturation. The peak of ~14.6 Å does not identify as a single mineral, and hence could be expandable/collapsible mixed-layer 2:1 minerals (MLMs). There was a peak at ~10.1 Å in all three treatments (i.e. of clay  $\text{Mg}_{\text{gly}}$ ,  $\text{K}_{\text{air}}$ , and  $\text{K}_{550}$ ) and at ~4.99 and ~3.34 Å in  $\text{Mg}_{\text{gly}}$ , which were the first-, second-, and third-order diffractions of illite, respectively. However, the peak at ~10.1 Å in  $\text{K}_{550}$  was due to illite and the collapsed MLMs. The dominant peak in  $\text{Mg}_{\text{gly}}$  at ~7.2 Å was also present in  $\text{K}_{\text{air}}$  but disappeared after heating to 550°C. Moreover, no peak at ~14.4 Å indicated the absence of any discrete vermiculite or chlorite, which could have generated a second-order peak at ~7.2 Å. Hence, the ~7.2 Å peak was due to kaolinite (001), and the relative peak area suggested that this was the dominant mineral in the iron oxide-free clay fraction of the red soil, as also reported earlier (Das et al., 2019a). Besides, minor quantities of feldspars and quartz were present, as evidenced by the minor peaks at ~6.3 and ~4.2 Å, respectively.

The XRD pattern of  $\text{Mg}_{\text{gly}}$  from the black soil showed a broad peak between 15 and 17 Å, which subdued and shifted to lower  $d$  spacings after K saturation ( $\text{K}_{\text{air}}$ ), but disappeared after heating ( $\text{K}_{550}$ ) (Fig. 4). The  $\text{Mg}_{\text{gly}}$  peak at ~10.2 Å intensified significantly after K saturation and heating ( $\text{K}_{550}$ ). Hence, the peak between 15 and 17 Å in  $\text{Mg}_{\text{gly}}$  was due to smectite and smectite-rich 2:1 mixed-layer minerals (Sm-MLMs) with interlayers accessible to  $\text{K}^+$  from outside. Along with that, another peak at ~14.6 Å appeared like a hump on the right side of the broad peak. As for the red soil clays, this peak could also be due to MLMs. The small peak at ~10.2 Å and those at ~4.99 and ~3.34 Å in  $\text{Mg}_{\text{gly}}$  suggested the presence of illite. Two small peaks at ~10.9 and ~10.6 Å, which diminished after K saturation and heating, could be due to illite-rich 2:1 interstratified minerals (IIMs). The black soil clays also contained a minor amount of chlorite, as evidenced by the peaks at ~14.1 Å (chlorite 001), ~7.04 Å (chlorite 002) in  $\text{K}_{550}$ , and ~4.7 Å (chlorite 003) in  $\text{Mg}_{\text{gly}}$ . The peaks at ~7.2 and ~3.6 Å in  $\text{Mg}_{\text{gly}}$  could be contributed by the 001 and 002 planes of kaolinite, respectively. The peak at ~3.34 Å was due to a small quantity of quartz (101) as well as illite (003).

The  $\text{Mg}_{\text{gly}}$  of the alluvial soil clay showed a small peak at ~19.0 Å and a more prominent peak at ~14.6 Å, both of which disappeared in the  $\text{K}_{550}$  with the intensification of ~10.1 Å peak (Fig. 5). Hence, these were MLMs capable of fixing  $\text{K}^+$  in the interlayers, which collapsed upon heating after K saturation. A sharp and dominant peak at ~10.1 Å along with minor peaks at ~4.99 and ~3.34 Å in  $\text{Mg}_{\text{gly}}$  revealed the dominance of illite in the clay fraction. The peak at ~7.2 Å in  $\text{Mg}_{\text{gly}}$  and  $\text{K}_{\text{air}}$ , and ~3.6 Å in  $\text{Mg}_{\text{gly}}$  indicated the

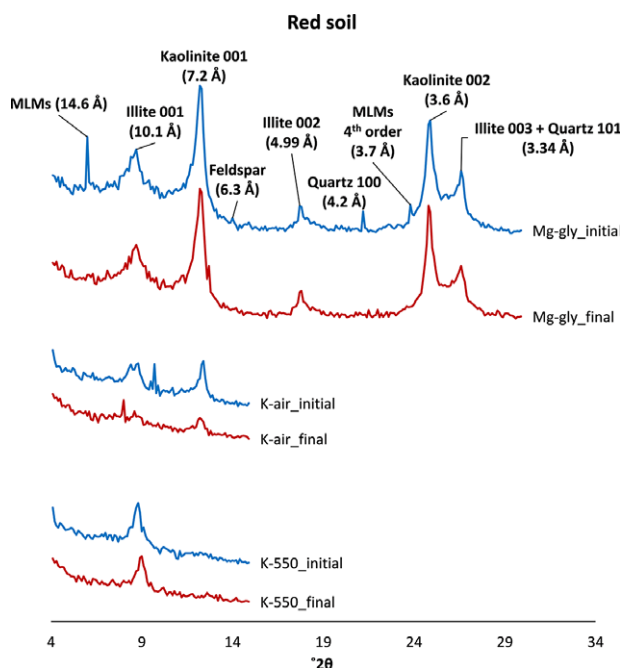


**Figure 3.** XRD patterns of the  $Mg_{gly}$ ,  $K_{air}$ , and  $K_{550}$  clay specimens of red soil before and after the leaching experiment.

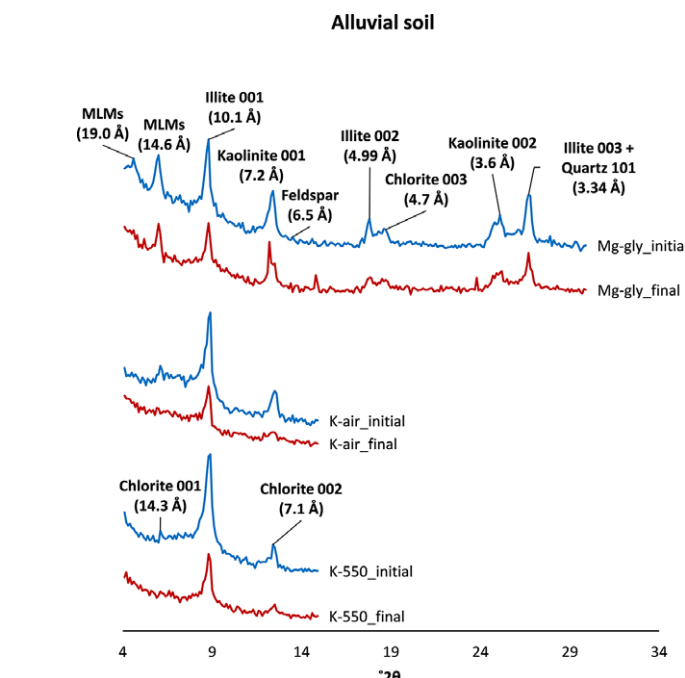


**Figure 5.** XRD patterns of the  $Mg_{gly}$ ,  $K_{air}$ , and  $K_{550}$  clay specimens of alluvial soil before and after the leaching experiment.

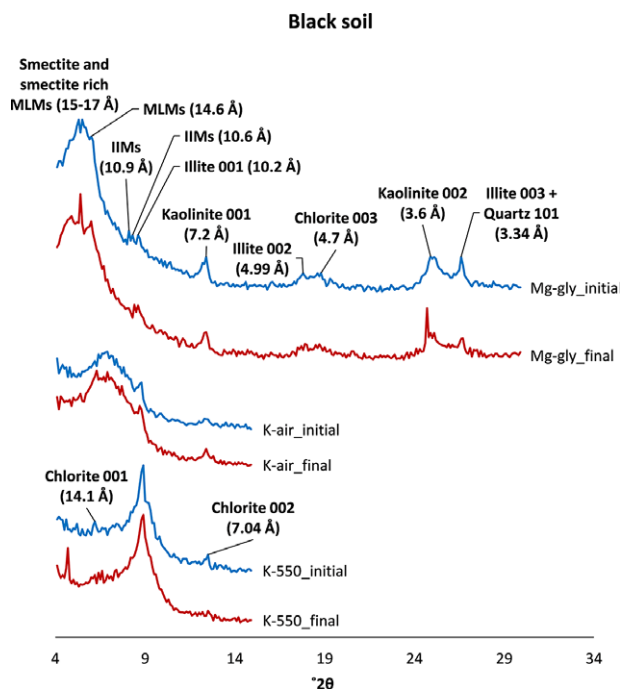


**Figure 4.** XRD patterns of the  $Mg_{gly}$ ,  $K_{air}$ , and  $K_{550}$  clay specimens of black soil before and after the leaching experiment.

presence of kaolinite. Minor peaks at  $\sim 14.3$  and  $\sim 7.1$  Å in  $K_{550}$ , and at  $\sim 4.7$  Å in  $Mg_{gly}$  indicated small amounts of chlorite. Small amounts of feldspars ( $\sim 6.5$  Å) and quartz ( $\sim 3.34$  Å) were also present.

#### Changes in clay minerals due to potassium depletion

The XRD patterns of clay specimens, especially of  $Mg_{gly}$  and  $K_{air}$ , of initial and final soils indicated alterations in the clay assemblages

due to K depletion upon  $60\times$  leaching (Figs 3–8). Relative peak areas do not show mineral abundance, but changes in these areas reveal mineral-abundance changes in specific soil clays.

The  $Mg_{gly}$  clay of initial red soil generated five component peaks at 14.6, 10.8, 10.2, 7.5, and 7.2 Å with relative peak areas of <1, <1, 30.6, 28.7, and 40.4%, respectively (Fig. 6a). The K-depleted red soil clay ( $Mg_{gly}$ ) showed no peak at 14.6 Å; had a smaller area under 7.7 Å (18.8%) than a similar peak in the initial soil clay (i.e. 28.7% under 7.5 Å), and slightly larger area under 7.2 Å (47.4%) than the initial soil clay (40.4%) (Fig. 6b). The final soil clay showed minor peaks at 12.3 Å (<1%), 10.3 Å (<1%), and 6.9 Å (1.2%), which were not present in the initial soil clay. The relative area under the illite peak remained almost the same after  $60\times$  leaching.

In black soil clay ( $Mg_{gly}$ ), the relative area under peaks occurring at 18.0–18.4 Å and 14.7–14.9 Å increased from 17.0 to 24.5% and from 55.9 to 61.7%, respectively, after  $60\times$  leaching (Fig. 7). The relative area under the peak from 16.5–16.7 Å declined noticeably from 17.5 to 4.8%. However, the sum of relative areas under smectite, Sm-MLMs, and other MLMs remained almost the same after  $60\times$  leaching. The initial soil clay ( $Mg_{gly}$ ) showed three peaks near 10.1 Å (i.e. 10.8, 10.6, and 10.2 Å), indicating illite and IIMs with a total relative area of 4%. The two peaks in similar positions (10.5 and 10.2 Å) in the final soil clay ( $Mg_{gly}$ ) contributed to a total relative area of 3.5%. The relative area under kaolinite (7.2 Å) remained virtually unchanged after  $60\times$  leaching (Fig. 7).

Initially, the alluvial soil clay ( $Mg_{gly}$ ) showed two peaks of MLMs at 19.0 and 14.7 Å with relative areas of 9.3 and 15.9%, respectively (Fig. 8a). Peaks at similar positions, i.e. 19.4 and 14.6 Å, had smaller relative areas of 2.6 and 14.3%, respectively, in the final soil clay (Fig. 8b). In addition, the final soil clay had two more peaks, at 18.3 and 16.8 Å, indicating MLMs, which were absent in the initial soil clay. After  $60\times$  leaching, the relative area under illite was reduced from 44.1 to 36%. The sum of relative areas under peaks at  $\sim 7.2$  Å was increased from 30.6 to 38.1% after  $60\times$  leaching. The peak at  $\sim 6$  Å might be due to the third-order diffraction of the  $\sim 18$  Å peak.

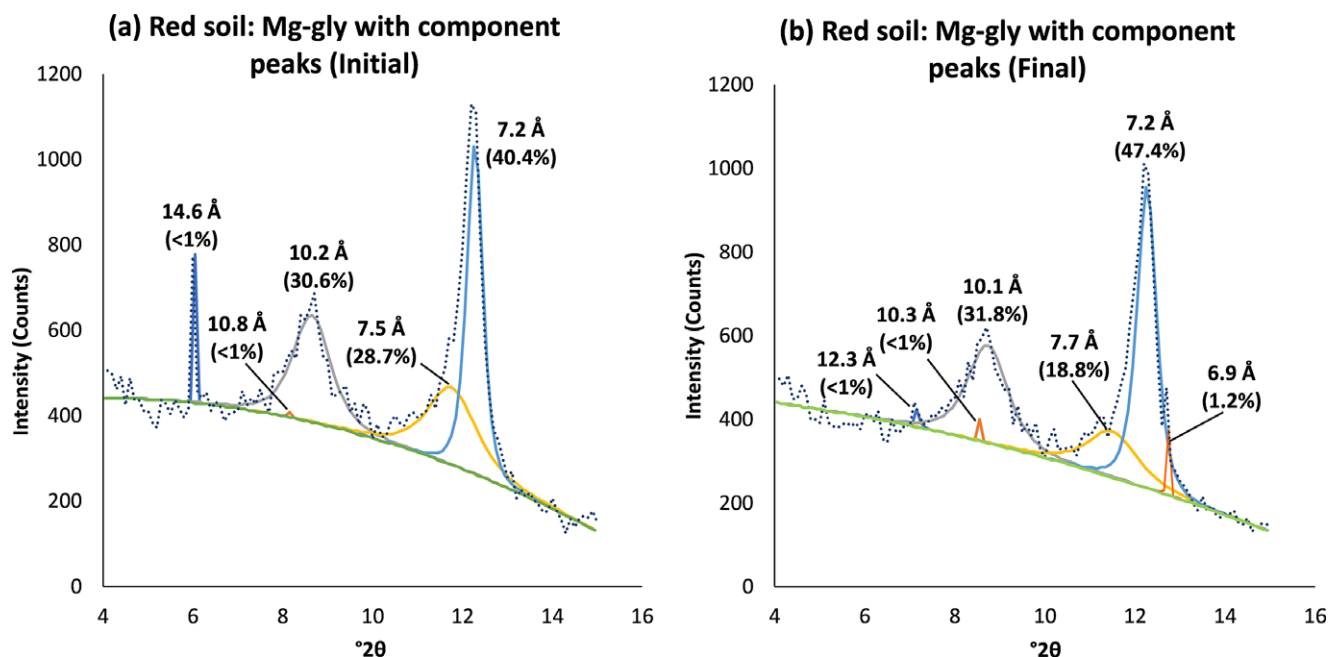


**Figure 6.** Red soil: (a) deconvoluted  $Mg_{gly}$  peaks before the leaching experiment; (b) deconvoluted  $Mg_{gly}$  peaks after the leaching experiment; the dotted curve in each figure is the observed  $Mg_{gly}$  XRD pattern, while the continuous curves represent the component peaks obtained after deconvolution; values within parentheses indicate relative areas under the corresponding peaks.

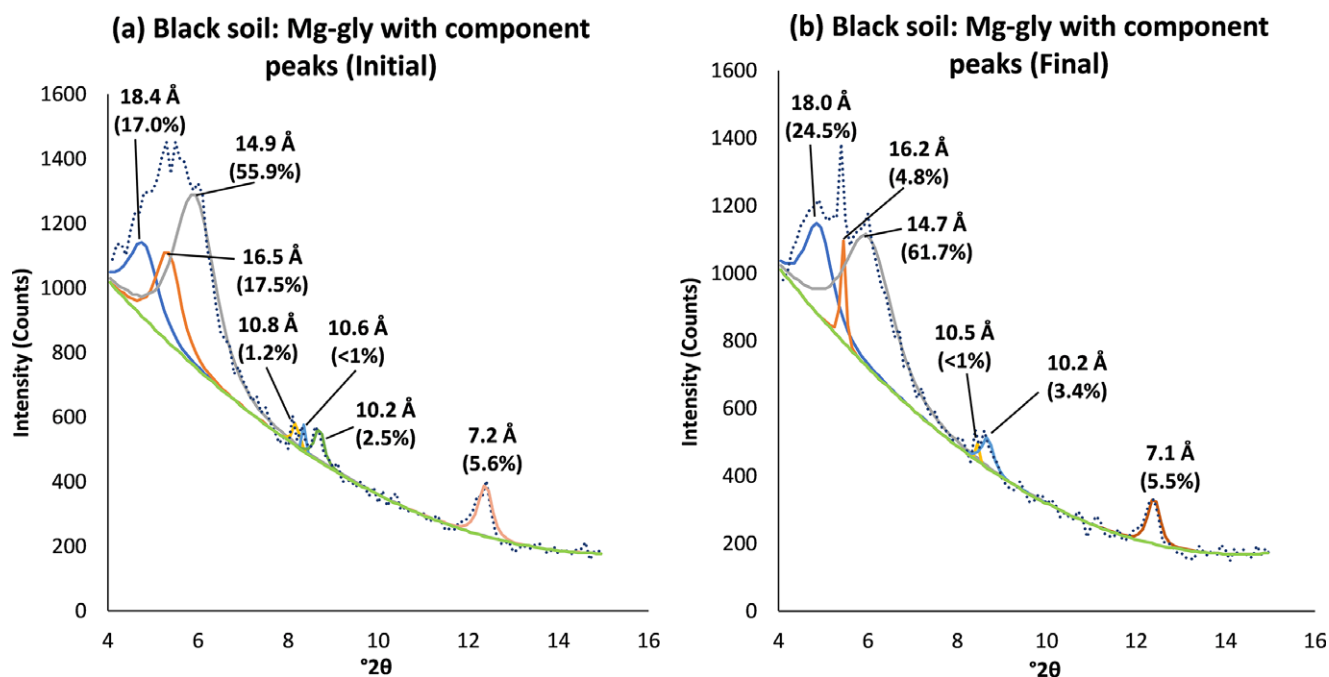


**Figure 7.** Black soil: (a) deconvoluted  $Mg_{gly}$  peaks before the leaching experiment; (b) deconvoluted  $Mg_{gly}$  peaks after the leaching experiment; the dotted curve in each figure is the observed  $Mg_{gly}$  XRD pattern, while the continuous curves represent the component peaks obtained after deconvolution; values within parentheses indicate relative areas under the corresponding peaks.

The X-ray intensity ratio of peak heights of basal reflections from 001 and 002 planes of illite (001/002) was reduced by leaching in all three soils due to K depletion (Table 3). The greatest reduction was in black soil (35.1%), followed by alluvial soil (18.6%), and then red soil (7.4%). Clay specimens of K-depleted soils showed slightly smaller  $c_g$  values than initial soils, e.g.  $c_g$  values of 1.018, 1.55, and 1.22 after 60× leaching compared with 1.024, 1.57, and 1.23 of the

initial soil clays for red, black, and alluvial soils, respectively (Table 3), which is the opposite to what one would expect.

#### *K*-fixation capacity

The black soil showed the greatest K-fixation capacity (initial value, 628 mg kg<sup>-1</sup>), followed by alluvial (initial value, 335 mg kg<sup>-1</sup>) and

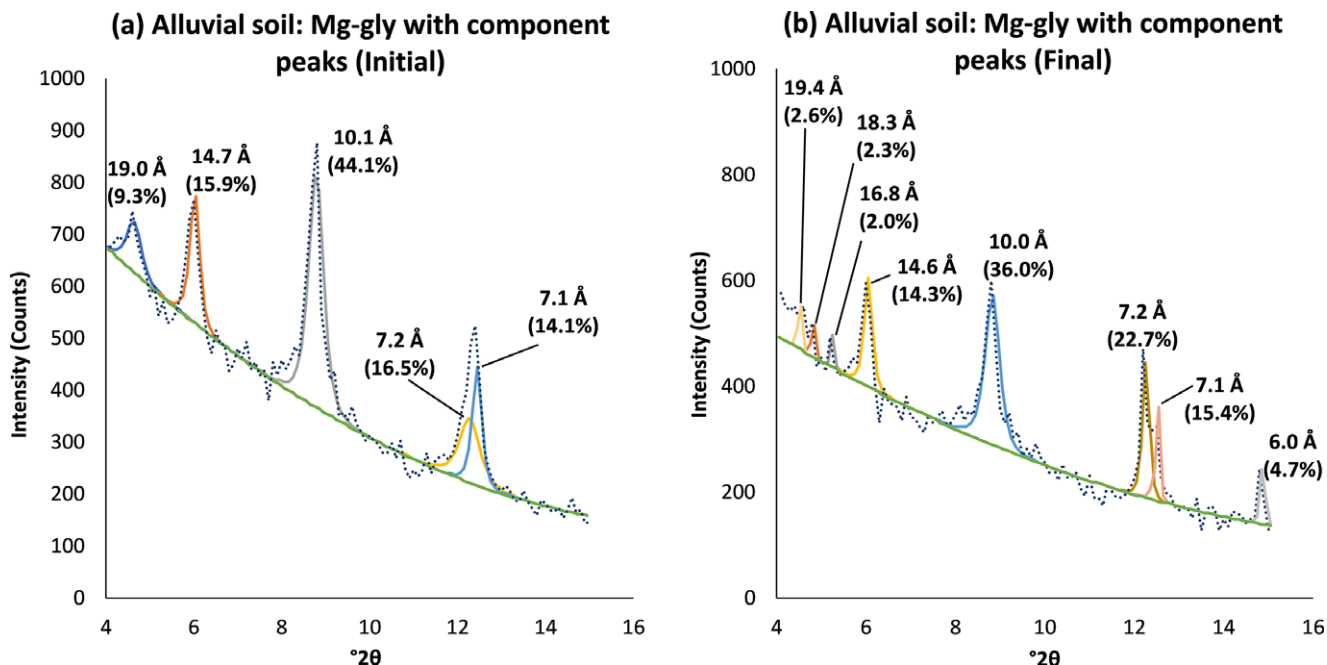


**Figure 8.** Alluvial soil: (a) deconvoluted  $Mg_{gly}$  peaks before the leaching experiment; (b) deconvoluted  $Mg_{gly}$  peaks after the leaching experiment; the dotted curve in each figure is the observed  $Mg_{gly}$  XRD pattern, while the continuous curves represent the component peaks obtained after deconvolution; values within parentheses indicate relative areas under the corresponding peaks.

**Table 3.** X-ray intensities of 001 and 002 planes of illite and their ratio

Soil		Peak intensity of illite 001*	Peak intensity of illite 002	001/002	cg
Red	Initial <sup>†</sup>	266	164	1.62	1.024
	Final	253	169	1.50 (↓7.4%)	1.018
Black	Initial	79	42	1.88	1.570
	Final	99	81	1.22 (↓35.1%)	1.550
Alluvial	Initial	449	182	2.47	1.230
	Final	289	144	2.01 (↓18.6%)	1.220

\*Peak intensities above background as obtained from  $Mg_{gly}$  diffractograms;

<sup>†</sup>Initial = before leaching experiment; Final = after 60× leaching; cg = center of gravity of the XRD peaks of the 2:1 clay minerals.

red (initial value, 168  $mg\ kg^{-1}$ ) soils (Fig. 9). The K-fixation capacity was increased significantly due to K-depletion in red (by 36.3%) and alluvial (by 20.6%) soils, but not in the black soil (Fig. 9; Table 2).

## Discussion

### K released from three soils

Potassium release from soil depends on its distribution across various pools, the extractant, and extraction time. In the field, plant uptake decreases soil solution K, which is buffered by K adsorbed on exchange sites. The exchangeable pool, and sometimes the solution pool, is replenished by K from the non-exchangeable pool, such as K in the interlayers of 2:1 minerals (Biliias and Barbayiannis, 2019; Das et al., 2022). Releases driven by plant uptake mainly occur through cation exchange reactions, where  $K^+$  on soil solids is replaced by  $H_3O^+$  from plant roots or  $Ca^{2+}$

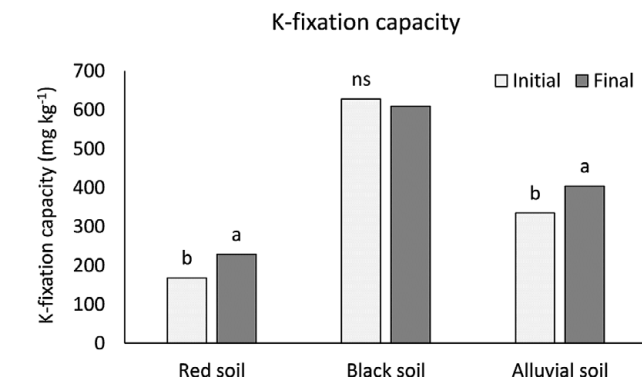


**Figure 9.** K-fixation capacity in 'initial' (before 60× leaching) and 'final' (after 60× leaching) soils; for a given soil, 'initial' and 'final' columns with different lower case letters indicate significant ( $p < 0.05$ ) difference between 'initial' and 'final' soils based on paired *t*-test (two-tailed); ns = non-significant ( $p > 0.05$ ). Comparison was not made among the three soils.

or  $Mg^{2+}$  in the soil solution. Thus, understanding soil K release via cation exchange provides insight into soil K-supplying ability. In this study, soils were leached successively with 1 M  $CaCl_2$  solution without shaking to prevent soil-particle disturbance, supplying  $Ca^{2+}$  for exchange with  $K^+$ . The use of such a high concentration of  $CaCl_2$  (i.e. 1 M) was intended to deplete K rapidly by driving the forward reaction through the increased concentration of one of the reactants.

The initial high K release from all soils (Fig. 1) resulted from K in the soil solution and on non-specific adsorption sites. Once these sources were depleted, the  $K^+-Ca^{2+}$  exchange front reached the edge (e-site)/wedge (w-site) sites of 2:1 minerals, reducing the K release rate. Further extraction caused the exchange front to access interlayers, further slowing the release. The rapid initial release involved K loosely bound to planar sites, followed by a slower

release of K more tightly bound to edge/wedge or interlayer sites (Shakeri and Abtahi, 2020; Hashemi and Najafi-Ghiri, 2024). Potassium ions were replaced from planar sites by  $\text{Ca}^{2+}$  diffused from the inner solution of soil colloids into the bulk solution for plant uptake or leaching (as in the present study). When K release occurred from edge/wedge or interlayer sites,  $\text{K}^+$  ions were first liberated within the clay matrix before diffusing to the bulk solution (Das et al., 2018). This process slowed K release, as  $\text{Ca}^{2+}$  struggles to enter the edge/wedge and interlayers of 2:1 minerals due to its larger hydrated diameter and faces difficulty in replacing K held there due to greater adsorption energy and greater specificity toward  $\text{K}^+$ . Interestingly, K release was similar for all soils after ~34 extractions, indicating that beyond a certain threshold, K release was independent of soil type, i.e. the sites that released K beyond a specific limit offered similar bonding energies for holding  $\text{K}^+$  irrespective of soil type.

The black soil had much greater K release, whereas the red soil showed significantly less total K release than the other two. The difference in K release among the three soils was mainly created during the first 16 extractions, when it was mostly contributed by soil solution and surface adsorbed (non-specific) pools. The black soil's much greater initial  $\text{NH}_4\text{OAc-K}$  led to greater initial and total K release compared with the other soils. Although  $\text{NH}_4\text{OAc-K}$  was greater in red soil than in calcareous alluvial soil, the latter released more total K over 60 extractions. A close look at K-release data (Fig. 1a) revealed that the difference between red and calcareous alluvial soils in total K released mainly occurred during the first three extractions and between the 25th and 34th extractions, after both soils reached a relatively constant K release rate. The initial lower K release from red soil compared with calcareous alluvial soil might stem from some  $\text{NH}_4\text{OAc-K}$  not exchanging with  $\text{Ca}^{2+}$ , even at zero  $\text{K}^+$  activity, known as minimum exchangeable K (Schneider et al., 2016). Although  $\text{NH}_4\text{OAc-K}$  was greater in red soil, its minimum exchangeable K, probably greater than that in calcareous alluvial soil, could have limited K release during  $\text{Ca}^{2+}$  exchange. Besides, K-bearing 2:1 minerals (e.g. illite or hydrous mica, illite-rich interstratified minerals) in soil might contain zones with varying expansion and layer charge (Shakeri and Abtahi, 2020). Between the 25th and 34th extractions, the  $\text{K}^+-\text{Ca}^{2+}$  exchange front probably accessed these zones with lower charge and greater expansion in calcareous alluvial soil, resulting in greater K release than from other soils. Another reason could be the greater proportion of trioctahedral illite in calcareous alluvial soil, as shown by the 001/002 values (Table 3). Trioctahedral mica (or illite) releases K more easily than dioctahedral mica (or illite). Pal et al. (2012) even suggested that K release from dioctahedral mica is unlikely when trioctahedral mica co-exists. Thus, the NEK released during 60× leaching probably came from trioctahedral mica (or illite) and IIMs. However, changes in clay minerals as observed from deconvoluted  $\text{Mg}_{\text{gly}}$  patterns indicated which minerals contributed to K release. Among the three soils, black soil probably had the greatest, while red soil had the lowest potential to supply K to plants, assuming that plants absorb K equally from each soil. However, the actual K availability may vary in the field due to multiple influencing factors, e.g. type of the crop and its duration, availability of other nutrients, climatic conditions, irrigation and other management practices, etc.

#### Changes in $\text{NH}_4\text{OAc-K}$ , $\text{NEK-HNO}_3$ , and $\text{NEK-NaTPB}$

The  $\text{NH}_4\text{OAc-K}$  pool consists of K in soil solution and that non-specifically adsorbed (adsorbed as hydrated  $\text{K}^+$  ions forming outer-

sphere complexes) on soil colloid surfaces (e.g. on planar i.e. p-sites of phyllosilicates, or on negatively charged organic colloids), making it readily available to plants (Das et al., 2022). In the present study, this pool was highly sensitive to K depletion, showing significant reductions across three soil types. However, its contribution to total K release was small: 4.3% in red soil, 17% in black soil, and 6.1% in calcareous alluvial soil. The black soil had the greatest  $\text{NH}_4\text{OAc-K}$  content, explaining its larger contribution to total K release than the other two soils. Despite this, most of the released K came from slowly releasable, reserve pools, highlighting their importance during intense K removal. Generally, NEK plays a key role in releasing K in soils with low  $\text{NH}_4\text{OAc-K}$  (Yanai et al., 2023), narrow differences between exchangeable and minimum exchangeable K (Das et al., 2019a; Das et al., 2021), abundant K-fixing minerals (Biliias and Barbayiannis, 2019), or extensive K depletion without input (Das et al., 2021; Das et al., 2022). Although minimum exchangeable K was not measured, other conditions applied, making non-exchangeable sources responsible for 83–95.7% of total K release in all soils.

The NEK pool in soil consists of K held in the interlayers of 2:1 clay minerals such as mica (or illite), vermiculite, and intergrade minerals. In the present study, NEK was estimated using both the boiling nitric acid ( $\text{HNO}_3$ ) method (Page et al., 1982) and the NaTPB method with a 5 min extraction time (Cox et al., 1999). While 5 min is insufficient to extract all interlayer K, it provides a good estimate of the plant-available NEK (Cox et al., 1999; Wang et al., 2016). Cox et al. (1999) even found it to be a better test for K availability than the  $\text{NH}_4\text{OAc}$  method. Although >80% of the total K released in the black soil (and >90% in other soils) came from sources other than soil solution and surface-adsorbed K, the  $\text{NEK-HNO}_3$  did not change significantly after 60× leaching. In contrast,  $\text{NEK-NaTPB}$  was more sensitive to K depletion than  $\text{NEK-HNO}_3$ , showing a significant decline in two of the three soils. As noted by Li et al. (2015),  $\text{NEK-HNO}_3$  does not just release K from the interlayers of 2:1 minerals via cation exchange; ~12–14% may come from mineral dissolution. Boiling  $\text{HNO}_3$  could break down some clay minerals or dissolve small feldspar particles (Bell et al., 2021a; Chen et al., 2023).  $\text{NEK-NaTPB}$  releases >99% of K through cation exchange (Li et al., 2015), explaining its greater sensitivity to K depletion from  $\text{CaCl}_2$  leaching. Despite this, changes in  $\text{NH}_4\text{OAc-K}$ ,  $\text{NEK-HNO}_3$ , and  $\text{NEK-NaTPB}$  combined explained ≤37% of total K released, probably because these methods extracted only a portion of the total NEK reserves. Nonetheless, K release from illite and MLMs led to changes in the clay mineral composition across all soils.

#### Changes in clay minerals

The withdrawal of reserve K during 60× leaching led to noticeable changes in the clay minerals of the soils, as seen in the  $\text{Mg}_{\text{gly}}$ ,  $\text{K}_{\text{air}}$ , and  $\text{K}_{550}$  XRD patterns (Figs 3–5). Deconvolution of  $\text{Mg}_{\text{gly}}$  patterns allowed crude quantification (as clay mineralogy was studied with composite samples rather than each replication separately) of the changes through relative peak area and *cg* values, while peaks at ~10.1 and ~4.99 Å provided the 001/002 values. Although relative peak areas do not correspond to exact mineral mass proportions, shifts in peak areas before and after K depletion indicate changes in mineral abundance (Moterle et al., 2019; Yanai et al., 2023). The *cg* is inversely related to the amount of anhydrous K layers in clay minerals (Moore and Reynolds, 1997). Generally, K removal from soils increases *cg* by raising the proportion of expanding 2:1 clay minerals (e.g. smectite, vermiculite, or mixed-layer minerals) at the

expense of mica (or illite) (Paola et al., 2016; Li et al., 2017b). Additionally, K release from dioctahedral mica (or illite) is unlikely in the presence of trioctahedral mica (or illite) due to the stronger K–O bond in the ditrigonal cavities of the former (Pal, 2017; Das et al., 2022). A 001/002 ratio near 1 indicates only dioctahedral components, while a ratio >1 indicates both di- and trioctahedral components of mica (or illite). Both contribute to the first-order peak (~10.1 Å), but only a dioctahedral component contributes to the second-order peak (~4.99 Å), with a trioctahedral contribution being negligible. As the trioctahedral proportion increases, the ratio grows. Soils with the same mica or illite content but a greater 001/002 ratio are believed to have better K-supplying ability for plants (Pal et al., 2001).

In red soil, changes in relative peak areas in the deconvoluted  $M_{\text{gly}}$  pattern indicated K release from MLMs (14.6 Å) and from the mineral assemblage represented by peaks at ~7.5–7.7 Å. These peaks (~7.5–7.7 Å) might be caused by interstratified kaolinite-smectite or by poorly crystallized kaolinite, as found in Brazil's subtropical red soils (Bortoluzzi et al., 2008; Moterle et al., 2016; Moterle et al., 2019). Alternatively, it could suggest the presence of illite alongside kaolinite and expanding type 2:1 minerals, with minute illite crystals observed with kaolinite in an Oxisol from Thailand (Darunsontaya et al., 2012). In the red soil, the relative area of illite and IIMs remained unchanged, with a slight increase from 30.9 to 31.9% considered negligible. In contrast, the calcareous alluvial soil experienced a significant drop from 44.1 to 36%, while black soil showed a moderate decrease from 4 to 3.5% in the relative area of illite or illite + IIMs due to K depletion. This differential response can be attributed to the weathering stages of the soils, with red soil (an Alfisol) being the most weathered and calcareous alluvial soil (an Entisol) the least. Previous studies suggest that a mineral phase's weathering history influences K availability more than its mere presence (Sanyal et al., 2014; Majumdar et al., 2017). Notably, an Entisol exhibited greater availability of K than an Alfisol in West Bengal, India despite similar illite content (Sanyal et al., 2014). Moreover, the initial 001/002 ratio and its decline due to K depletion were least in red soil, indicating a smaller proportion of trioctahedral mica (or illite) and reflecting its more advanced weathering stage compared to the other soils (Table 3). As weathering advances, illite in the clay fraction becomes more dioctahedral in character (Pal et al., 2001).

In black soil, the broad peak of Sm-MLMs split into two peaks at 16.5 Å and 18.4 Å, which shifted to 16.2 Å and 18.0 Å, respectively, due to K depletion. The relative area under the 18–18.4 Å peak increased at the expense of the 16.2–16.5 Å peak, indicating that the Sm-MLMs represented by the latter contributed to K release during 60 × leaching with CaCl<sub>2</sub> besides illite+IIMs. Illite and smectite, along with their MLMs could buffer soil K (Velde and Peck, 2002; Jindaluang and Darunsontaya, 2024). Extended K removal due to crop demand leads to the depletion of K in 2:1 clay minerals (Firmano et al., 2020; Yanai et al., 2023). Over time, K might be released from residual mica fragments occluded within the crystalline framework of kaolinite or 2:1–1:1 MLMs (Firmano et al., 2020). The significant K release from Sm-MLMs compared to illite + IIMs in black soil is attributed to the smaller amount of the latter, as indicated by changes in relative peak areas. In calcareous alluvial soil, K release was primarily from illite, with some contribution from MLMs peaking at ~14.6 Å as shown by changes in relative areas under different peaks. Potassium removal from illite interlayers expanded the layers, generating multiple MLM peaks above 14.6 Å, enhancing the smectitic nature of the clay assemblage. The relative area of peaks at ~7.2 Å

increased from 30.5% to 38.1% with K depletion, indicating kaolinite-type mineral enrichment or higher-order diffractions of smectite-rich MLMs.

The 001/002 ratios indicated that illite in the red soil was primarily dioctahedral, while the calcareous alluvial soil contained a significant trioctahedral component, with an intermediate level in black soil (Table 3). According to Pal et al. (2001), the decline in 001/002 due to K depletion was linked solely to K release from trioctahedral components. Dioctahedral mica (muscovite) might not release K in the presence of trioctahedral mica (biotite), as even small amounts of K can inhibit its release (Rausell-Colom et al., 1965; Pal et al., 2001). Thus, illite's contribution to K release in black and calcareous alluvial soils was probably due to the trioctahedral component, as indicated by reductions in 001/002. In this study, the decline in the 001/002 ratio did not correlate proportionally with changes in the relative areas of illite or illite + IIMs. For example, the 001/002 ratio decreased by 7.4% in red soil, while there was no change in illite + IIMs' relative area. In black soil, the ratio dropped by 35.1%, corresponding to only a 10% reduction in illite + IIMs' relative area. In calcareous alluvial soil, the 001/002 ratio decreased by 18.6%, with an 18.1% reduction in illite's relative area. Additionally, Sm-MLMs along with illite + IIMs contributed to K release in black soil, while illite was mainly responsible in calcareous alluvial soil. Further research is needed to understand the factors affecting the 001/002 ratio to better evaluate clay minerals' impact on soil K-supplying ability. The lack of replicated data might also explain the disproportionate changes in the 001/002 ratio and the relative peak areas of illite + IIMs, which highlights a limitation of this study.

In the present study, the *cg* did not follow the expected trend of increasing with K depletion, as observed by several previous researchers (Barré et al., 2007; Paola et al., 2016; Li et al., 2017b). Instead, *cg* decreased slightly in all three soils after K depletion, although the decrease was negligible. This minor change might have resulted from insufficient K depletion to cause a noticeable impact on *cg*. Additionally, the lack of replicated data from the deconvoluted XRD patterns may explain the minimal differences observed even after 60× leaching. It is also possible that *cg* is not a reliable indicator of soil K reserves. Further research is needed to assess the effectiveness of *cg* in evaluating soil K reserves and the associated changes due to K depletion.

### K-fixation capacity

The black soil exhibited the greatest total K release and K-fixation capacity, probably due to its clay content being more than twice that of the other soils. Large clay contents with 2:1 clay minerals correlates with strong K-releasing and fixation abilities (Bell et al., 2021b). A notable decrease in NEK-NaTPB, indicating K release from 2:1 minerals led to increased K fixation in red and calcareous alluvial soils. However, the black soil's K-fixation capacity remained unchanged like its NEK-NaTPB after 60× leaching, probably due to its already high initial K-fixation capacity. Das et al. (2018) found that NP fertilization led to significantly greater K-fixation capacity than NPK after 45 years of rice-rice cropping in an alluvial soil (Aeric Endoaquept) from eastern India. In the present study, the increase in K-fixation capacity with respect to the K released from pools other than the NH<sub>4</sub>OAc-K (i.e. water-soluble and exchangeable) was 34.5 and 37.2% in the red and calcareous alluvial soils, respectively, and –9.5% in the black soil. The K addition for the K-fixation capacity determination was 1000 mg kg<sup>-1</sup>, >20× the general recommendation for K fertilization in India. Based on this,

it appeared that K depletion from the red and the calcareous alluvial soil could only be partly (<40%) reversed through addition of K. However, no such inference could be drawn for the black soil.

Besides K depletion, the continuous wetting period over the 60× leaching and the ten wetting–drying cycles used in K-fixation capacity determination probably impacted the soils differently due to redox cycles, as their clay mineralogy varied significantly (Shen and Stucki, 1994). The iron-free clay fraction of the red, alluvial, and black soils was dominated by kaolinite, illite, and smectite, respectively. Different responses of clay minerals towards K-fixation and release due to redox were seen earlier (Khaled and Stucki, 1991; Shen and Stucki, 1994). Moist conditions leading to reduction of structural Fe<sup>3+</sup> tended to increase the surface charge and K-fixing ability of smectites, whereas re-oxidation upon drying or exposure to oxygen decreased the same. Multiple redox cycles increased the proportion of Fe<sup>2+</sup> and K-fixation ability of smectites. In contrast, reduction of Fe<sup>3+</sup> in illite decreases its K-fixation ability. As Fe<sup>3+</sup> converts to Fe<sup>2+</sup> in the octahedral sheet of illite, the dipole moment of OH<sup>-</sup> tilts along the *c*-axis, weakening the attraction between the negatively charged clay surface and K<sup>+</sup> ions (Juo and White, 1969; Shen and Stucki, 1994). The 60× leaching period and 10 wetting–drying cycles during K-fixation capacity testing in this study probably altered the redox environment of all three soils. Hence, observed differences in K-fixation capacity of the three soils and the change after 60× leaching were not only due to inherent differences in clay content, mineralogy and K-depletion, but also due to the differential response of different clay minerals to redox cycles.

### Is 60× leaching enough to induce ‘long-term cultivation’-like changes in soil K and clay minerals?

The relative change in NH<sub>4</sub>OAc-K due to K-depletion upon 60× leaching was comparable to, and the changes in NEK-HNO<sub>3</sub> and NEK-NaTPB were lower than, that observed in similar soils after 41–42 years of cultivation with NP fertilization without K (Das, 2018; Das et al., 2019a; Das et al., 2021). However, even with 60× leaching in the laboratory, significant change was observed in NH<sub>4</sub>OAc-K in all soils and NEK-NaTPB in two soils, leading to notable shifts in K-fixation capacity in two soils and changes in clay mineral composition in all three soils. The 60× leaching was not sufficient to induce changes to match four decades of intensive cultivation in the field (as observed by Das, 2018; Das et al., 2019a; Das et al., 2021), but it gave some quantitative indication of the ill effects of continuous K-depletion on the soil K-status. Future studies should compare the effects of varying laboratory leaching periods on soil K-related variables and clay minerals with those observed in the field after different cultivation periods. This will help to determine the amount of leaching needed to induce field-like changes associated with specific cropping cycles or years.

### Conclusions

The constant rate of K release for a given extractant did not vary from one soil to another. Changes in non-exchangeable K measured using sodium tetraphenyl borate with 5 min extraction time were better correlated than that achieved by measuring using the conventional boiling nitric acid method to changes in the K-fixation capacity of soils. Besides illite and illite-rich mixed-layer minerals (peaked at or near 10.1 Å), smectite-rich mixed-layer minerals and other 2:1 mixed-layer minerals could contribute

to K release under continuous removal. The ratio of peak intensities for the first-order and second-order diffraction of illite (001/002) decreased with K depletion, but this change was not proportional to the decrease in the relative abundance of illite. The center of gravity of the XRD peaks of 2:1 clay minerals (*cg*) did not indicate the soil's K reserves consistently, as it did not increase with K depletion in any of the three soils; 60× leaching of soils with 1 M CaCl<sub>2</sub> partially simulated the changes in K-related variables and clay minerals induced by long-term cultivation without K fertilization. Future studies should establish a reliable laboratory method to simulate changes in soil K-related variables and clay minerals seen in the field after long-term cultivation without K fertilization. In addition, a detailed investigation of the 001/002 ratio of illite or mica and the *cg* is needed to better understand their relationship with soil K depletion or enrichment.

**Supplementary material.** The supplementary material for this article can be found at <http://doi.org/10.1017/cmn.2025.6>.

**Author contributions.** Debarup Das: Conceptualization, Data curation, Formal analysis, Investigation, Methodology, Visualization, Writing – original draft, Writing – review & editing, Writing – revised version; Mandira Barman: Conceptualization, Investigation, Methodology, Resources, Supervision, Writing – review & editing.

**Acknowledgements.** The authors are grateful to the Director, ICAR-Indian Agricultural Research Institute, New Delhi, for access to the facilities used in the study.

**Financial support.** The research work was supported by an *In-House* project named ‘Restoration and Improvement of Soil Health’ (Institute Code: NRMAIARISIL201402/CRSCIARISIL2014025257) of ICAR-Indian Agricultural Research Institute, New Delhi.

**Competing interests.** The authors declare that they have no known competing financial interests or personal relationships that could have appeared to influence the work reported in this paper.

**Data availability statement.** Data generated in the present study have been presented in the paper as tables and figures.

### References

- Barman, M., & Das, D. (2024). Nitric acid and organic acid mixture show less deviation in extractability of potassium between field-moist and air-dried soil. *Communications in Soil Science and Plant Analysis*, 55, 1028–1040. <https://doi.org/10.1080/00103624.2023.2290003>
- Barré, P., Velde, B., Catel, N., & Abbadie, L. (2007). Soil–plant potassium transfer: impact of plant activity on clay minerals as seen from X-ray diffraction. *Plant and Soil*, 292, 137–146. <https://doi.org/10.1007/s11104-007-9208-6>
- Bell, M.J., Thompson, M.L., & Moody, P.W. (2021a). Using soil tests to evaluate plant availability of potassium in soils. In *Improving Potassium Recommendations for Agricultural Crops* (ed. T.S. Murrell, R.L. Mikkelsen, G. Sulewski, R. Norton, & M.L. Thompson), pp. 191–218. Springer, Switzerland. [https://doi.org/10.1007/978-3-030-59197-7\\_8](https://doi.org/10.1007/978-3-030-59197-7_8)
- Bell, M.J., Thompson, M.L., & Moody, P.W. (2021b). Considering soil potassium pools with dissimilar plant availability. In *Improving Potassium Recommendations for Agricultural Crops* (ed. T.S. Murrell, R.L. Mikkelsen, G. Sulewski, R. Norton, & M.L. Thompson), pp. 163–190. Springer, Switzerland. [https://doi.org/10.1007/978-3-030-59197-7\\_7](https://doi.org/10.1007/978-3-030-59197-7_7)
- Bilias, F., & Barbayiannis, N. (2017). Evaluation of sodium tetraphenylboron (NaBPh<sub>4</sub>) as a soil test of potassium availability. *Archives of Agronomy and Soil Science*, 63, 468–476. <https://doi.org/10.1080/03650340.2016.1218479>
- Bilias, F., & Barbayiannis, N. (2019). Potassium-fixing clay minerals as parameters that define K availability of K-deficient soils assessed with a modified Mitscherlich equation model. *Journal of Soil Science and Plant Nutrition*, 19, 830–840. <https://doi.org/10.1007/s42729-019-00082-3>

- Bortoluzzi, E.C., Velde, B., Pernes, M., Dur, J.C., & Tessier, D. (2008). Vermiculite, with hydroxy-aluminium interlayer, and kaolinite formation in a subtropical sandy soil from south Brazil. *Clay Minerals*, 43, 185–193. <https://doi.org/10.1180/claymin.2008.043.2.03>
- Bouyoucos, G.J. (1962). Hydrometer method improved for making particle size analysis of soils. *Agronomy Journal*, 54, 464–465. <https://doi.org/10.2134/agronj1962.00021962005400050028x>
- Carey, P.L., & Metherell, A.K. (2003). Rates of release of nonexchangeable potassium in New Zealand soils measured by a modified sodium tetraphenyl-boron method. *New Zealand Journal of Agricultural Research*, 46, 185–197. <https://doi.org/10.1080/00288233.2003.9513546>
- Chen, Y.L., Huang, L., Cheng, L.J., Liu, Z.J., & Xue, B. (2023). Straw returning and potassium fertilization affect clay mineralogy and available potassium. *Nutrient Cycling in Agroecosystems*, 126, 195–211. <https://doi.org/10.1007/s10705-023-10284-y>
- Cheng, M., Bell, R., Brown, J., Ma, Q., & Scanlan, C. (2023). Comparison of soil analytical methods for estimating plant-available potassium in highly weathered soils. *Soil Research*, 61, 717–733. <https://doi.org/10.1071/SR22270>
- Cox, A.E., Joern, B.C., Brouder, S.M., & Gao, D. (1999). Plant-available potassium assessment with a modified sodium tetraphenylboron method. *Soil Science Society of America Journal*, 63, 902–911. <https://doi.org/10.2136/sssaj1999.634902x>
- Darunsontaya, T., Suddhiprakarn, A., Kheoruenromne, I., Prakongkep, N., & Gilkes, R.J. (2012). The forms and availability to plants of soil potassium as related to mineralogy for upland Oxisols and Ultisols from Thailand. *Geoderma*, 170, 11–24. <https://doi.org/10.1016/j.geoderma.2011.10.002>
- Das, D. (2018). *Effect of long-term fertilization and manuring on potassium dynamics in soils of varying mineralogical make-up*. PhD thesis, ICAR- Indian Agricultural Research Institute, New Delhi, India. <https://krishikosh.egranth.ac.in/handle/1/5810092870>
- Das, D., & Datta, S.C. (2019). Identification and semi-quantification of soil minerals by X-ray diffraction analysis. In *Soil Analysis* (ed. S.K. Singh, D.R. Biswas, C.A. Srinivasamurthy, S.P. Datta, G. Jayasree, P. Jha, S.K. Sharma, R. N. Katkar, K.P. Raverkar, & A.K. Ghosh), pp. 583–600. Indian Society of Soil Science, New Delhi, India.
- Das, D., Datta, S.C., & Sahoo, S. (2019b). Determination of cation exchange capacity of soil. In *Soil Analysis* (ed. S.K. Singh, D.R. Biswas, C.A. Srinivasamurthy, S.P. Datta, G. Jayasree, P. Jha, S.K. Sharma, R.N. Katkar, K.P. Raverkar, & A.K. Ghosh), pp. 87–104 Indian Society of Soil Science, New Delhi, India.
- Das, D., Dwivedi, B.S., Datta, S.P., Datta, S.C., Meena, M.C., Agarwal, B.K., Shahi, D.K., Singh, M., Chakraborty, D., & Jaggi, S. (2019a). Potassium supplying capacity of a red soil from eastern India after forty-two years of continuous cropping and fertilization. *Geoderma*, 341, 76–92. <https://doi.org/10.1016/j.geoderma.2019.01.041>
- Das, D., Dwivedi, B.S., Datta, S.P., Datta, S.C., Meena, M.C., Dwivedi, A.K., Singh, M., Chakraborty, D., & Jaggi, S. (2021). Long-term differences in nutrient management under intensive cultivation alter potassium supplying ability of soils. *Geoderma*, 393, 14983. <https://doi.org/10.1016/j.geoderma.2021.114983>
- Das, D., Nayak, A.K., Thilagam, V.K., Chatterjee, D., Shahid, M., Tripathi, R., Mohanty, S., Kumar, A., Lal, B., Gautam, P., & Panda, B.B. (2018). Measuring potassium fractions is not sufficient to assess the long-term impact of fertilization and manuring on soil's potassium supplying capacity. *Journal of Soils and Sediments*, 18, 1806–1820. <https://doi.org/10.1007/s11368-018-1922-6>
- Das, D., Sahoo, J., Raza, M.B., Barman, M., & Das, R. (2022). Ongoing soil potassium depletion under intensive cropping in India and probable mitigation strategies: a review. *Agronomy for Sustainable Development*, 42, 4. <https://doi.org/10.1007/s13593-021-00728-6>
- Datta, S.C. (1996). Characterization of micaceous minerals in soils for strain and size of crystallites through deconvolution and curve fitting of XRD profile. *Clay Research*, 15, 20–27.
- Datta, S.C., Ghosh, S.K., & Das, D. (2020). Soil mineralogy and clay minerals. In *The Soils of India* (ed. B.B. Mishra), pp. 109–127. World Soils Book Series, Springer, Cham. [https://doi.org/10.1007/978-3-030-31082-0\\_6](https://doi.org/10.1007/978-3-030-31082-0_6)
- Firmano, R.F., Melo, V.F., Montes, C.R., Junior, A.O., Castro, C., & Alleoni, L.R. F. (2020). Potassium reserves in the clay fraction of a tropical soil fertilized for three decades. *Clays and Clay Minerals*, 68, 237–249. <https://doi.org/10.1007/s42860-020-00078-6>
- Han, T., Huang, J., Liu, K., Fan, H., Shi, X., Chen, J., Jiang, X., Liu, G., Liu, S., Zhang, L., Xu, Y., Feng, G., & Zhang, H. (2021). Soil potassium regulation by changes in potassium balance and iron and aluminum oxides in paddy soils subjected to long-term fertilization regimes. *Soil and Tillage Research*, 214, 105168. <https://doi.org/10.1016/j.still.2021.105168>
- Hanway, J.J., & Heidel, H. (1952). Soil analysis methods as used in Iowa State College Soil Testing Laboratory. *Iowa Agriculture*, 57, 1–13.
- Hashemi, S.S., & Najafi-Ghiri, M. (2024). Kinetic of potassium release from vermiculite clay soil to calcium chloride and citric acid solutions (emphasis on clay mineralogy changes). *Communications in Soil Science and Plant Analysis*, 55, 782–795. <https://doi.org/10.1080/00103624.2023.2277412>
- Jackson, B.L.J. (1985a). A modified sodium tetraphenylboron method for the routine determination of reserve-potassium status of soil. *New Zealand Journal of Experimental Agriculture*, 13, 253–262. <https://doi.org/10.1080/03015521.1985.10426091>
- Jackson, M.L. (1973). *Methods of Chemical Analysis*. Prentice Hall of India, New Delhi, India.
- Jackson, M.L. (1985b). *Soil Chemical Analysis: Advanced Course*, 2nd edn. University of Wisconsin, Madison, USA.
- Jindaluang, W., & Darunsontaya, T. (2024). Role of soil organic carbon composition on potassium availability in smectite-dominated paddy soils. *Journal of Soil Science and Plant Nutrition*, 24, 1288–1300. <https://doi.org/10.1007/s42729-024-01631-1>
- Juo, A.S.R., & White, J.L. (1969). Orientation of the dipole moments of hydroxyl groups in oxidized and unoxidized biotite. *Science*, 165, 804–805. <https://doi.org/10.1126/science.165.3895.804>
- Kassambara, A. (2023). *rstatix: Pipe-Friendly Framework for Basic Statistical Tests*. <https://CRAN.R-project.org/package=rstatix>
- Khaled, E.M., & Stucki, J.W. (1991). Effects of iron oxidation state on cation fixation in smectites. *Soil Science Society of America Journal*, 55, 550–554.
- Li, J., Niu, L., Zhang, Q., Di, H., & Hao, J. (2017a). Impacts of long-term lack of potassium fertilization on different forms of soil potassium and crop yields on the North China Plains. *Journal of Soils and Sediments*, 17, 1607–1617. <https://doi.org/10.1007/s11368-017-1658-8>
- Li, T., Wang, H., Chen, X., & Zhou, J. (2017b). Soil reserves of potassium: release and availability to *Lolium perenne* in relation to clay minerals in six cropland soils from Eastern China. *Land Degradation and Development*, 28, 1696–1703. <https://doi.org/10.1002/ldr.2701>
- Li, T., Wang, H., Zhou, Z., Chen, X., & Zhou, J. (2015). A nano-scale study of the mechanisms of non-exchangeable potassium release from micas. *Applied Clay Science*, 118, 131–137. <https://doi.org/10.1016/j.clay.2015.09.013>
- Liu, K., Han, T., Huang, J., Shah, A., Li, D., Yu, X., Huang, Q., Ye, H., Hu, H., Hu, Z., & Zhang, H. (2020). Links between potassium of soil aggregates and pH levels in acidic soils under long-term fertilization regimes. *Soil and Tillage Research*, 197, 104480. <https://doi.org/10.1016/j.still.2019.104480>
- Majumdar, K., Sanyal, S.K., Singh, V.K., Dutta, S., Satyanarayana, T., & Dwivedi, B.S. (2017). Potassium fertiliser management in Indian agriculture: current trends and future needs. *Indian Journal of Fertilisers*, 13, 20–30.
- Mehra, O.P., & Jackson, M.L. (1960). Iron oxide removal from soils and clay by a dithionite-citrate system buffered with sodium bicarbonate. *Clays and Clay Minerals*, 7, 317–327. <http://doi.org/10.1346/CCMN.1958.0070122>
- Mendiburu, F. (2023). *agricolae: Statistical Procedures for Agricultural Research*. <https://CRAN.R-project.org/package=agricolae>
- Moore, D.E., & Reynolds, R.C. (1997). *X-Ray Diffraction and the Identification of Clay Minerals*, 2nd edn. Oxford University Press, New York, USA.
- Moterle, D.F., Bortoluzzi, E.C., Kaminski, J., Rheinheimer, D.S., & Caner, L. (2019). Does Ferralsol clay mineralogy maintain potassium long-term supply to plants? *Revista Brasileira de Ciência do Solo*, 43, e0180166. <https://doi.org/10.1590/18069657rbc20180166>
- Moterle, D.F., Kaminski, J., Rheinheimer, D.S., Caner, L., & Bortoluzzi, E.C. (2016). Impact of potassium fertilization and potassium uptake by plants on soil clay mineral assemblage in South Brazil. *Plant and Soil*, 406, 157–172. <https://doi.org/10.1007/s11104-016-2862-9>

- Najafi-Ghiri, M., Boostani, H.R., & Hardie, A.G. (2023). Release of potassium from some heated calcareous soils to different solutions. *Archives of Agronomy and Soil Science*, 69, 90–103. <https://doi.org/10.1080/03650340.2021.1958321>
- Najafi-Ghiri, M., Rezabigi, S., Hosseini, S., Boostani, H.R., & Owliaie, H.R. (2019). Potassium fixation of some calcareous soils after short term extraction with different solutions. *Archives of Agronomy and Soil Science*, 65, 897–910. <https://doi.org/10.1080/03650340.2018.1537485>
- Page, A.L., Miller, R.H., & Keeney, D.R. (1982). *Methods of Soil Analysis (Part II): Chemical and Microbiological Properties*, 2nd edn. Agronomy Society of America, Madison, Wisconsin.
- Pal, D.K. (2017). *A Treatise of Indian and Tropical Soils*. Springer, Cham. <https://doi.org/10.1007/978-3-319-49439-5>
- Pal, D.K., Bhattacharyya, T., Chandran, P., & Ray, S.K. (2012). Linking minerals to selected soil bulk properties and climate change: a review. *Clay Research*, 31, 38–69.
- Pal, D.K., Srivastava, P., Durge, S.L., & Bhattacharyya, T. (2001). Role of weathering of fine-grained micas in potassium management of Indian soils. *Applied Clay Science*, 20, 39–52. [https://doi.org/10.1016/S0169-1317\(01\)00044-8](https://doi.org/10.1016/S0169-1317(01)00044-8)
- Paola, A., Pierre, B., Vincenza, C., Di, M.V., & Bruce, V. (2016). Short term clay mineral release and re-capture of potassium in a *Zea mays* field experiment. *Geoderma*, 264, 54–60. <https://doi.org/10.1016/j.geoderma.2015.10.005>
- Paul, S., Das, D., Barman, M., Verma, B.C., Sinha, A.K., & Datta, A. (2024). Selection of a suitable extractant for sequential leaching of soil to evaluate medium-term potassium availability to plants. *Journal of Soil Science and Plant Nutrition*, 24, 1489–1506. <https://doi.org/10.1007/s42729-024-01654-8>
- Portela, E., Monteiro, F., Fonseca, M., & Abreu, M.M. (2019). Effect of soil mineralogy on potassium fixation in soils developed on different parent material. *Geoderma*, 343, 226–234. <https://doi.org/10.1016/j.geoderma.2019.02.040>
- Prasad, J., Nagaraju, M.S.S., & Naidu, M.V.S. (2019). Mechanical analysis of soil by international pipette and hydrometer. In *Soil Analysis* (ed. S.K. Singh, D.R. Biswas, C.A. Srinivasamurthy, S.P. Datta, G. Jayasree, P. Jha, S.K. Sharma, R. N. Katkar, K.P. Raverkar, & A.K. Ghosh), pp. 249–266 Indian Society of Soil Science, New Delhi, India.
- Rausell-Colom, J.A., Sweatman, T.R., Wells, C.B., & Norrish, K. (1965). Studies in the artificial weathering of mica. In *Experimental Pedology* (ed. E.G. Hallsworth, & D.V. Crawford), pp. 40–72. Butterworths, London, UK.
- Sanyal, S.K., Majumdar, K., & Singh, V.K. (2014). Nutrient management in Indian agriculture with special reference to nutrient mining – a relook. *Journal of the Indian Society of Soil Science*, 62, 307–325.
- Schneider, A., Augusto, L., & Mollier, A. (2016). Assessing the plant minimal exchangeable potassium of a soil. *Journal of Plant Nutrition and Soil Science*, 179, 584–590. <https://doi.org/10.1002/jpln.201600095>
- Shakeri, S., & Abtahi, A. (2020). Potassium fixation capacity of some highly calcareous soils as a function of clay minerals and alternately wetting-drying. *Archives of Agronomy and Soil Science*, 66, 445–457. <https://doi.org/10.1080/03650340.2019.1619176>
- Shen, S., & Stucki, J.W. (1994). Effects of iron oxidation state on the fate and behavior of potassium in soils. In *Soil Testing: Prospects for Improving Nutrient Recommendations* (ed. J.L. Havlin, & J. Jacobsen), pp. 173–185. Special Publication Number 40, Soil Science Society of America, Madison, Wisconsin. <https://doi.org/10.2136/sssaspecpub40.c10>
- Simonsson, M., Hillier, S., & Öborn, I. (2009). Changes in clay minerals and potassium fixation capacity as a result of release and fixation of potassium in long-term field experiments. *Geoderma*, 151, 109–120. <https://doi.org/10.1016/j.geoderma.2009.03.018>
- Srinivasarao, Ch., Reddy, S.B., & Kundu, S. (2014). Potassium nutrition and management in Indian agriculture. *Indian Journal of Fertilisers*, 10, 58–80.
- Sumner, M.E., & Miller, P.M. (1996). Cation exchange capacity and exchange coefficient. In *Methods of Soil Analysis: Part 3 Chemical Methods* (ed. D.L. Sparks, A.L. Page, P.A. Helmke, R.H. Loeppert, P.N. Soltanpour, M.A. Tabatabai, C.T. Johnston, & M.E. Sumner), pp. 1201–1229. Soil Science Society of America, Madison, WI, USA. <https://doi.org/10.2136/sssabookser5.3.c40>
- Velde, B., & Peck, T. (2002). Clay mineral changes in the Morrow experimental plots, University of Illinois. *Clays and Clay Minerals*, 50, 364–370. <https://doi.org/10.1346/000986002760833738>
- Walkley, A., & Black, I.A. (1934). An examination of the Degtjareff method for determining soil organic matter, and a proposed modification of the chromic acid titration method. *Soil Science*, 37, 29–38. <http://doi.org/10.1097/00010694-193401000-00003>
- Wang, H.Y., Cheng, W., Li, T., Jianmin, Z.H., & Xiaoqin, C.H. (2016). Can nonexchangeable potassium be differentiated from structural potassium in soils? *Pedosphere*, 26, 206–215. [https://doi.org/10.1016/S1002-0160\(15\)60035-2](https://doi.org/10.1016/S1002-0160(15)60035-2)
- Weil, R.R., & Brady, N.C. (2017). *The Nature and Properties of Soils*, 15th edn. Pearson Education, London.
- Yanai, J., Inoue, N., Nakao, A., Kasuya, M., Ando, K., Oga, T., Takayama, T., Hasukawa, H., Takehisa, K., Takamoto, A., Togami, K., & Takahashi, T. (2023). Use of soil nonexchangeable potassium by paddy rice with clay structural changes under long-term fertilizer management. *Soil Use and Management*, 39, 785–793. <https://doi.org/10.1111/sum.12862>